

7,12-Dimethylbenz[*A*]Anthracene Induces Sertoli–Leydig-Cell Tumors in the Follicle-Depleted Ovaries of Mice Treated with 4-Vinylcyclohexene Diepoxide

Zelieann R Craig,¹ John R Davis,² Samuel L Marion,³ Jennifer K Barton,⁴ and Patricia B Hoyer^{3,*}

Ovarian cancer is associated with high mortality due to its late onset of symptoms and lack of reliable screening methods for early detection. Furthermore, the incidence of ovarian cancer is higher in postmenopausal women. Mice rendered follicle-depleted through treatment with 4-vinylcyclohexene diepoxide (VCD) are a model of ovary-intact menopause. The present study was designed to induce ovarian neoplasia in this model by treating mice with 7,12-dimethylbenz[*a*]anthracene (DMBA). Female B6C3F1 mice (age, 28 d) received intraperitoneal sesame oil (vehicle; VCD– groups) as a control or VCD (160 mg/kg; VCD+ groups) daily for 20 d to cause ovarian failure. Four months after the onset of dosing, mice from each group received a single injection of DMBA (VCD–DMBA+ and VCD+DMBA+ groups, *n* = 15 per group) or vehicle control (VCD–DMBA–, *n* = 15; VCD+ DMBA–, *n* = 14) under the bursa of the right ovary. Ovaries were collected 3 or 5 mo after injection and processed for histologic evaluation. Immunohistochemistry was used to confirm classification of neoplasms. None of the animals in the VCD–DMBA– and VCD–DMBA+ groups (that is, mice still undergoing estrus) had tumors at either time point. At the 3-mo time point, 12.5% of the VCD+DMBA+ mice had ovarian tumors; at 5 mo, 57.1% of the VCD+DMBA+ and 14.3% of VCD+DMBA– ovaries had neoplasms. Neoplasms stained positively for inhibin α (granulosa cells) and negatively for keratin 7 (surface epithelium), thus confirming classification of the lesions as Sertoli–Leydig cell tumors. These findings provide evidence for an increased incidence of DMBA-induced ovarian neoplasms in the ovaries of follicle-depleted mice compared with that in age-matched cycling controls.

Abbreviations: DMBA, 7,12-dimethylbenz[*a*]anthracene; OSE, ovarian surface epithelium; VCD, 4-vinylcyclohexene diepoxide.

Approximately 20,000 women are diagnosed with ovarian cancer annually, of whom 15,000 are anticipated to die of the disease. Ovarian cancer ranks fifth in deaths by all cancers and first in cancers of the reproductive system.¹² The survival rate of ovarian cancer patients improves greatly when the disease is detected early,² but fewer than 20% of ovarian cancers are found at an early stage due to the lack of reliable screening methods for early detection. Because approximately two-thirds of ovarian cancer cases are diagnosed in women older than 55 y, the incidence of ovarian cancer is increased in peri- and postmenopausal women.¹² For this reason, research using relevant animal models of menopause is needed to advance the understanding of the biology of neoplasms in the postmenopausal ovary.

Ovarian cancer can be due to transformation of surface epithelial cells, germ cells, or sex cord and stromal cells. Almost 90% of all ovarian cancers are thought to be derived from the flat-to-cuboidal epithelial cells (that is, the ovarian surface epithelium [OSE]) that cover the ovary.^{6,49} Alternatively, fewer than 5% of ovarian cancers are classified as sex cord–stromal tumors, which include granulosa cell tumors, and Sertoli–Leydig cell tumors.¹⁸ The incidence of sex cord–stromal ovarian cancers is highest in

women older than 50 y, but has also been diagnosed in premenopausal women.¹⁸ The etiology of ovarian cancer is not completely understood, but factors associated with development of the disease include ovulation, altered levels of gonadotropins (luteinizing and follicle-stimulating hormones) and steroid hormones (estrogens and androgens), germ-cell or follicle depletion, altered expression of oncogenes and tumor suppressor genes, altered levels of growth factors and cytokines, and exposure to environmental agents.⁴¹

Recently, an ovary-intact mouse model of menopause was developed by using the occupational chemical 4-vinylcyclohexene diepoxide (VCD).^{24,25,27} Repeated daily dosing of mice and rats with VCD selectively destroys ovarian primordial and primary follicles by accelerating the natural process of follicular atresia.^{14,15,42,44} Because VCD does not target larger follicles, the animal continues to ovulate normally until no more follicles can be recruited. Thus, ovarian follicular depletion in the VCD-treated mouse is gradual. As with women undergoing perimenopause, VCD-treated mice show increased levels of follicle-stimulating hormone,²⁷ irregular estrous cycles, and declining levels of estrogen²⁴ as they become follicle-depleted. In addition, residual ovarian tissue is retained after ovarian failure. Therefore, preservation of residual ovarian tissue in the VCD-treated follicle-depleted mouse makes this model ideal for studying the physiology of the postmenopausal ovary. The VCD-treated mouse model of peri- and postmenopause has been used to study several menopause-related disorders including atherosclerotic lesion develop-

Received: 23 Sep 2009. Revision requested: 07 Oct 2009. Accepted: 21 Oct 2009.

¹Department of Veterinary Biosciences, University of Illinois, Urbana, Illinois; ²Department of Pathology, University Medical Center, ³Department of Physiology, Arizona Health Sciences Center, and ⁴Department of Biomedical Engineering, BIO5 Institute, University of Arizona, Tucson, Arizona.

*Corresponding author. Email: hoyer@u.arizona.edu

ment,²⁸ diabetic kidney disease,²⁰ osteoporosis,⁵¹ and metabolic syndrome.³⁹ Because the VCD-treated mouse has been shown to be relevant for studies related to both perimenopausal and postmenopausal stages,⁵⁰ it is a useful candidate for studies of ovarian cancer.

Even though spontaneous ovarian tumors in rodents have been reported,³⁶ the paucity of these cases precludes their use in modeling ovarian cancer. Therefore, much effort has been put into developing relevant animal models for ovarian cancers. One such model involves the use of the carcinogen 7,12-dimethylbenz[*a*]anthracene (DMBA),^{8,21,23,43} a polycyclic aromatic hydrocarbon that induces carcinogenic mutations by forming DNA adducts.⁹ Recently, the DMBA model of carcinogenesis has been combined with the VCD model of menopause to cause ovarian cancer in F344 rats.^{13,19} However, no studies have characterized the combined use of both chemicals in mice. Developing this combined model in mice is important because of the existence of various genetically engineered mice that have potential relevance to enhancing our understanding of the biology of ovarian cancer.

The present study was designed to determine whether ovarian failure affects susceptibility to the development of ovarian neoplasms in mice and to model DMBA-induced ovarian neoplasia in VCD-treated follicle-depleted mice. VCD-treated follicle-depleted mice and cycling controls received ovarian injections with DMBA to induce neoplasia. The incidence of neoplasms was determined by histologic evaluation, and the lesions were classified through immunostaining for keratin 7 and inhibin α .

Materials and Methods

Animals. Female B6C3F1 mice (age, 21 d) were purchased from Jackson Laboratories (Bar Harbor, ME). On arrival, mice were housed under SPF conditions in polycarbonate plastic cages at a room temperature of 22 ± 2 °C and on 12:12-h light:dark cycles and were fed ad libitum. Animals were certified free of *Mycoplasma pulmonis*, ecto- and endoparasites, and mouse hepatitis virus, minute virus of mice, mouse parvovirus, murine norovirus, rotavirus, Theiler murine encephalomyelitis virus, and Sendai virus. All mice were allowed to acclimate to the animal facilities for 1 wk before the start of the experiment. All experiments and methods were approved by the University of Arizona Institutional Animal Care and Use Committee and conformed to the *Guide for the Care and Use of Experimental Animals*.¹⁶

VCD-induced ovarian failure. Mice were allocated randomly into treatment groups and received daily intraperitoneal injections of VCD (in sesame oil; 160 mg/kg; Sigma–Aldrich, St Louis, MO) or sesame oil only (2.5 mL/kg; Sigma–Aldrich) for 20 d.

Intrabursal injections. Mice received intraperitoneal ketamine–xylazine (16 μ L/g body weight; Ketaject, Phoenix Pharmaceutical, St Joseph, MO, and AnaSed, Lloyd Pharmaceuticals, Shenandoah, IA), and anesthesia was defined by cessation of movement, recumbency, and lack of response to aversive stimulation of paw and tail. The right flank of each animal was shaved and the skin cleaned with povidone iodine and 70% ethanol. An incision was made through the skin, fascia, and abdominal wall, and the ovary was externalized. DMBA (in sesame oil; 50 μ g; Sigma–Aldrich) or an equivalent volume of sesame oil only (Sigma–Aldrich) was injected directly under the bursa, the thin membrane that surrounds the ovary. The muscle wall was closed by using 6-0 braided silk suture, and the skin was closed by using 3-0 braided silk suture. Surgical glue (Tissumend II, Veterinary Products Laboratories,

Phoenix, AZ) was applied over the incision to prevent reopening of the wound in case the sutures became undone. The left ovary was not injected and was used as an untreated contralateral control.

Tissue collection. Animals were euthanized by CO₂ inhalation followed by cervical dislocation. Both ovaries were dissected, trimmed of fat, and separately fixed in 4% formalin for subsequent embedding, sectioning, and staining.

Hematoxylin and eosin staining. Ovaries were trimmed, placed in 4% formalin for 4 h, transferred to 70% ethanol, and paraffin-embedded. Each ovary was sectioned (4 to 5 μ m) and mounted, and every 10th section was saved and stained with hematoxylin and eosin. Additional unstained ovarian sections were used for immunohistochemical staining.

Immunohistochemistry. Immunohistochemistry was performed by incubating sections in an automatic immunostainer (ES immunostainer, Ventana Medical Systems, Tucson, AZ) for 24 min. A keratin 7 stain (Dako, Carpinteria, CA) was used to label ovarian surface epithelial cells, and inhibin α (anti-inhibin clone R1, Dako) was used to stain steroidogenic sex-cord–stromal cellular components within tumors. Antibody application was followed by treatment with a biotin-conjugated goat antimouse antibody, avidin-D–conjugated horseradish peroxidase, and then 3',3'-diaminobenzidine tetrahydrochloride with copper enhancement as color substrate. Hematoxylin was used as the counterstain. After clearing in graded alcohols and xylene, slides were coverslipped. Dark brown structures indicated positive staining.

Statistical analysis. Data for the incidence of ovarian neoplasms were analyzed by using the Fisher exact test (SPSS Statistics v17.0, Chicago, IL), with significance set at a *P* value of less than 0.05.

Results

Incidence of ovarian neoplasms. The effect of direct application of vehicle or DMBA under the bursa of the right ovary of VCD-treated follicle-depleted mice and age-matched cycling controls was evaluated histologically at 3 or 5 mo after surgery (Figure 1). No tumors were identified in any of the cycling control mice (VCD–DMBA– and VCD–DMBA+ groups) at either time point. At 3 mo after injection, 1 of the 8 (12.5%) follicle-depleted mice that received DMBA (VCD+DMBA+ group) showed ovarian neoplasms in the injected (right) ovary. This number was increased to 4 of the 7 (57.1%) VCD+DMBA+ mice at 5 mo after injection. In comparison, 1 of the 7 (14.3%) VCD-treated follicle-depleted mice that received vehicle (VCD+DMBA– group) had ovarian neoplasia in the right ovary at the 5-mo time point. All ovarian tumors at the 5-mo time point occurred in the injected ovary. In addition, at 3 mo, there were 2 cases (1 each in the VCD+DMBA– and VCD+DMBA+ groups) of spontaneous (nonDMBA-induced) ovarian tumors in the contralateral, noninjected (left) ovary. Mice with neoplasms in the left ovary did not also have neoplasms in the right ovary and therefore were not included in the incidence data.

Morphologic features of ovaries. Sections from the ovaries of VCD-treated follicle-depleted mice and age-matched cycling controls collected at 3 and 5 mo after injection with vehicle or DMBA were stained with hematoxylin and eosin (Figures 2 to 4). At 3 mo, ovaries from VCD–DMBA– mice appeared normal, with evidence of ongoing folliculogenesis as demonstrated by the presence of preantral and antral follicles as well as corpora lutea and rare atretic follicles (Figure 2 A). In contrast, VCD–DMBA+

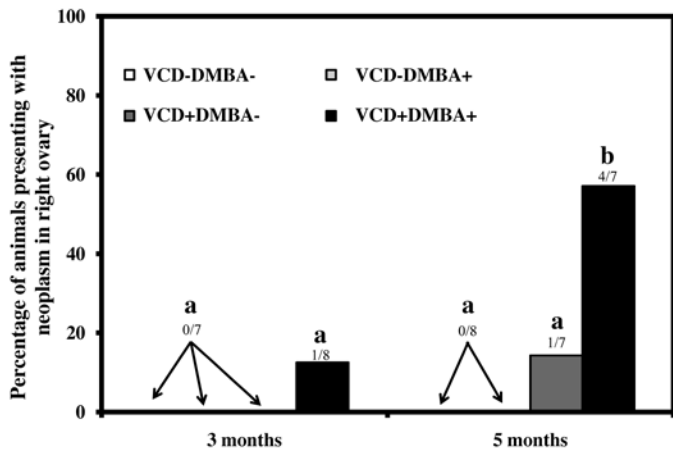


Figure 1. Incidence of ovarian neoplasms in VCD-treated follicle-depleted mice compared with age-matched cycling controls. Ovaries were removed 3 or 5 mo after injection and processed for histologic evaluation. Data are presented as percentage (%) of animals with neoplasms relative to the total number evaluated. The numbers over each bar represent the actual number of animals with neoplasms / actual total animals in the treatment group. Different letters indicate significant ($P < 0.05$; $n = 7$ to 8 per group) difference in incidence between groups.

ovaries showed markedly less folliculogenesis as evidenced by fewer follicles of all sizes, fewer corpora lutea, and more atretic follicles at both time points (Figure 2 B). At 5 mo after injection, VCD-DMBA+ ovaries showed no evidence of ovulation (no corpora lutea) and few follicles (Figure 2 C). As expected for follicle-depleted mice, VCD+DMBA- and VCD+DMBA+ ovaries showed no folliculogenesis and numerous luteinized stromal cells (Figure 2 D and E). Ovaries from VCD+DMBA+ mice in which neoplasms were identified showed predominant clusters of Sertoli-like and Leydig-like cells, aggregates of larger luteinized cells forming sex cord tumors of intermediate differentiation which, in some cases, replaced normal ovarian tissue (Figure 3 A through E). In addition, both ovaries of all VCD-treated mice had numerous invaginations of the OSE and outer cortex of the ovary (also known as ovarian epithelial hyperplasia and benign tubular adenomas;¹ Figure 4 A through C).

Immunohistochemical staining. Whereas OSE-derived cancers stain positive for the intermediate filament protein keratin 7, sex-cord-stromal tumors stain positive for inhibin α .²⁹ To facilitate classification of tumor origin, immunohistochemistry for inhibin α (Figure 5 A) and keratin 7 (Figure 5 B) was performed. Positive staining for inhibin α was particularly strong in Sertoli-like cells and weak or absent in Leydig-like cells, thus confirming classification of tumors as Sertoli-Leydig cell tumors (Figure 5 A). Further, all neoplasms were negative for keratin 7 (data not shown). OSE and tubular adenomas were positive for keratin 7 (Figure 5 B) and negative for inhibin α (data not shown).

Discussion

This study was designed to determine whether ovarian failure affects susceptibility to development of ovarian neoplasms in mice and to further characterize DMBA-induced ovarian neoplasia in the VCD-treated follicle-depleted mouse. To accomplish this goal, VCD-treated follicle-depleted mice and age-matched cycling controls received single unilateral intrabursal injections

of DMBA (or vehicle only as a control), and the incidence of neoplasms was determined. In the present study, a single direct application of DMBA into the intrabursal space of the right ovary of VCD-treated follicle-depleted mice resulted in neoplasms in 12.5% and 57.1% of the mice at 3 and 5 mo after injection, respectively, whereas no neoplasms were identified in the right ovary of either VCD-DMBA+ or VCD-DMBA- cycling controls (at 3 or 5 mo) or VCD+DMBA- mice (3 mo). In addition, spontaneous tumors were identified in the right ovary only and left ovary only of 2 individual VCD+DMBA- mice (at 5 mo and 3 mo, respectively) and in the left ovary of a VCD+DMBA+ mouse (at 3 mo).

We performed immunohistochemical analysis to assist in classification of the tumors observed in this study. Keratin 7 was used as a marker for the OSE, and inhibin α was used to label sex-cord-stromal tumors.²⁹ All neoplasms were positive for inhibin α (both Sertoli- and Leydig-like components) and negative for keratin 7 (only present in OSE). Therefore, together with the morphologic data obtained from histologic evaluation, immunohistochemistry confirmed that the neoplasms in our mice were Sertoli-Leydig-cell tumors. These tumors are members of the sex-cord-stromal tumor family, which represents fewer than 5% of ovarian cancers in women.^{18,22} Sertoli-Leydig-cell tumors have also been identified in VCD-treated follicle-depleted F344 rats treated with DMBA¹³ and aging follicle-stimulating-hormone receptor knockout mice with ovarian failure (FORKO mice).¹⁰ However, the present study is the first to describe the development of DMBA-induced Sertoli-Leydig-cell tumors in VCD-treated follicle-depleted wild-type mice.

Studies evaluating the DMBA model of ovarian carcinogenesis traditionally have focused on using rats rather than mice.^{8,13,19,43} However, the few reports available on overall DMBA-induced carcinogenesis in mice have shown reproducible ovarian neoplasms despite differences in methods of delivery (gavage versus coated suture), dosage, length of exposure, and length of time before collection of tissues. In one study, C57BL6/129Sv mice received daily doses of DMBA by gavage for 3 wk; 71% of animals developed granulosa cell tumors after 1 y.⁵ In another study, mice of a C57BL6/NCr;Sv129;FVB/NCr background received a weekly dose of DMBA by gavage for 6 wk; 6 mo after treatment, 27.3% (12 of 44) of mice developed ovarian neoplasms, of which 58% were granulosa cell tumors.³⁵ Recently, a study assessing the incidence of cancers in mice with a germline p53 mutation found that 80% of wild-type (AJ background) mice that received implants of DMBA-coated suture into their ovaries developed ovarian tumors, of which 50% were adenocarcinomas (malignant, epithelial-derived) when evaluated 3 mo after application of implants.⁴⁸

In the present study, none of the cycling animals exposed to DMBA developed ovarian neoplasms but rather experienced follicle loss. DMBA targets ovarian follicles of all types and causes premature ovarian failure.²⁶ Therefore, decreased folliculogenesis in VCD-DMBA+ mice in the current study is likely the result of ovotoxicity from the single intrabursal injection of DMBA that they received. In contrast, other studies have documented the presence of DMBA-induced tumors in ovaries of cycling mice.^{5,35,48} The reason for the lack of ovarian neoplasms in VCD-DMBA+ mice in the present study is not understood but may reflect the limited exposure to DMBA as compared with that of other studies. Perhaps neoplasms were more frequent in VCD+ mice because of the increased levels of luteinizing hormone (po-

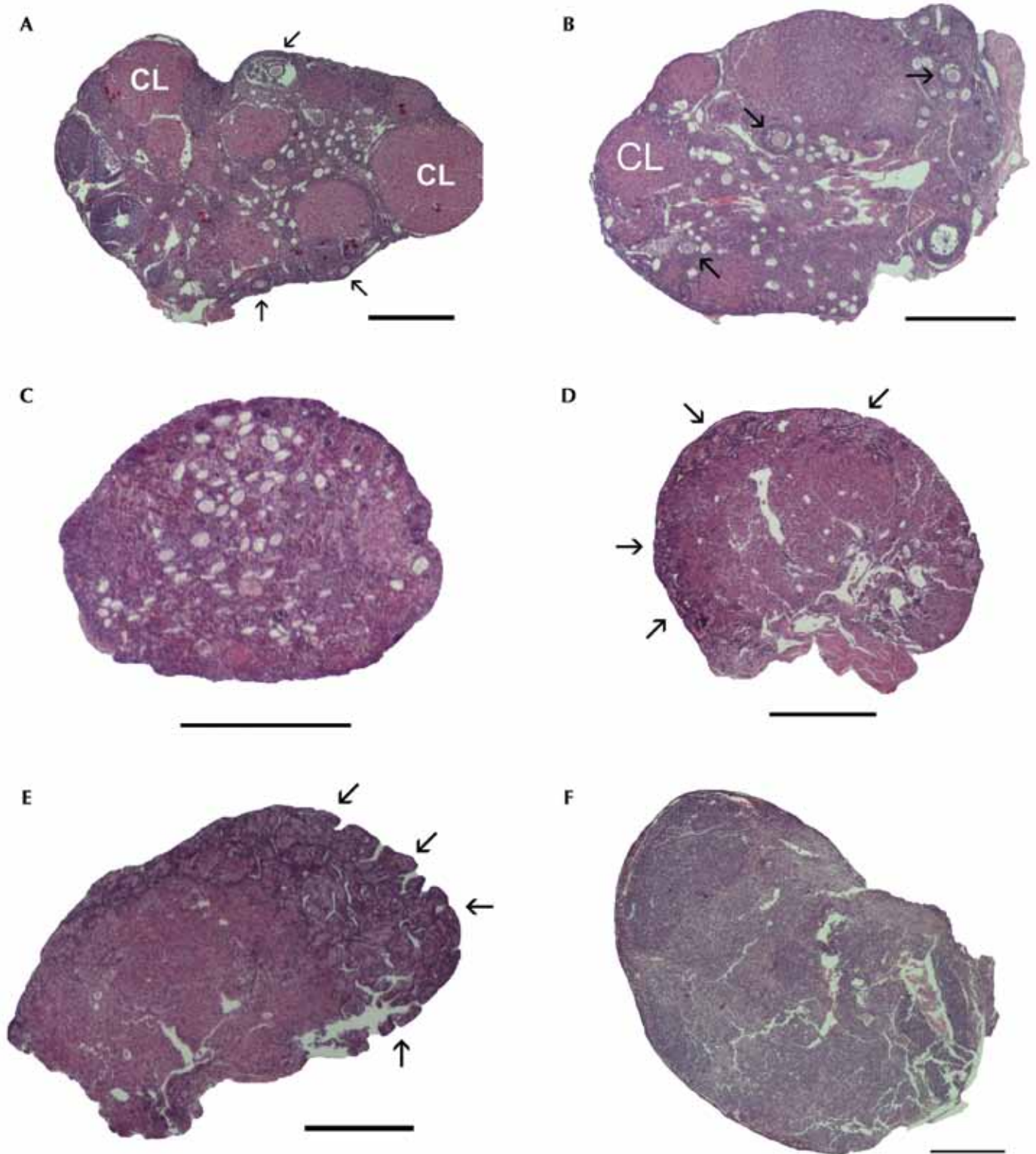


Figure 2. Ovaries collected at 3 and 5 mo after intrabursal injection with DMBA. Ovaries were removed 3 or 5 mo postinjection and processed for histological evaluation as described in Materials and Methods. (A) VCD-DMBA- ovary at 3 mo shows evidence of folliculogenesis (arrows, follicles) and ovulations (CL, corpus luteum). (B) VCD-DMBA+ ovary at 3 mo shows decreased number of follicles (arrows) and corpora lutea. (C) VCD-DMBA+ at 5 mo showing lack of follicles and corpora lutea. (D and E) VCD+DMBA- ovaries showing examples of tubular adenoma (black arrows) and luteinized stromal cells. (F) VCD+DMBA+ ovary showing a tumor that has replaced normal ovarian tissue. Hematoxylin and eosin stain; magnification, $\times 4$ (bar, 500 μm). Panels A and F were constructed by combining overlapping images.

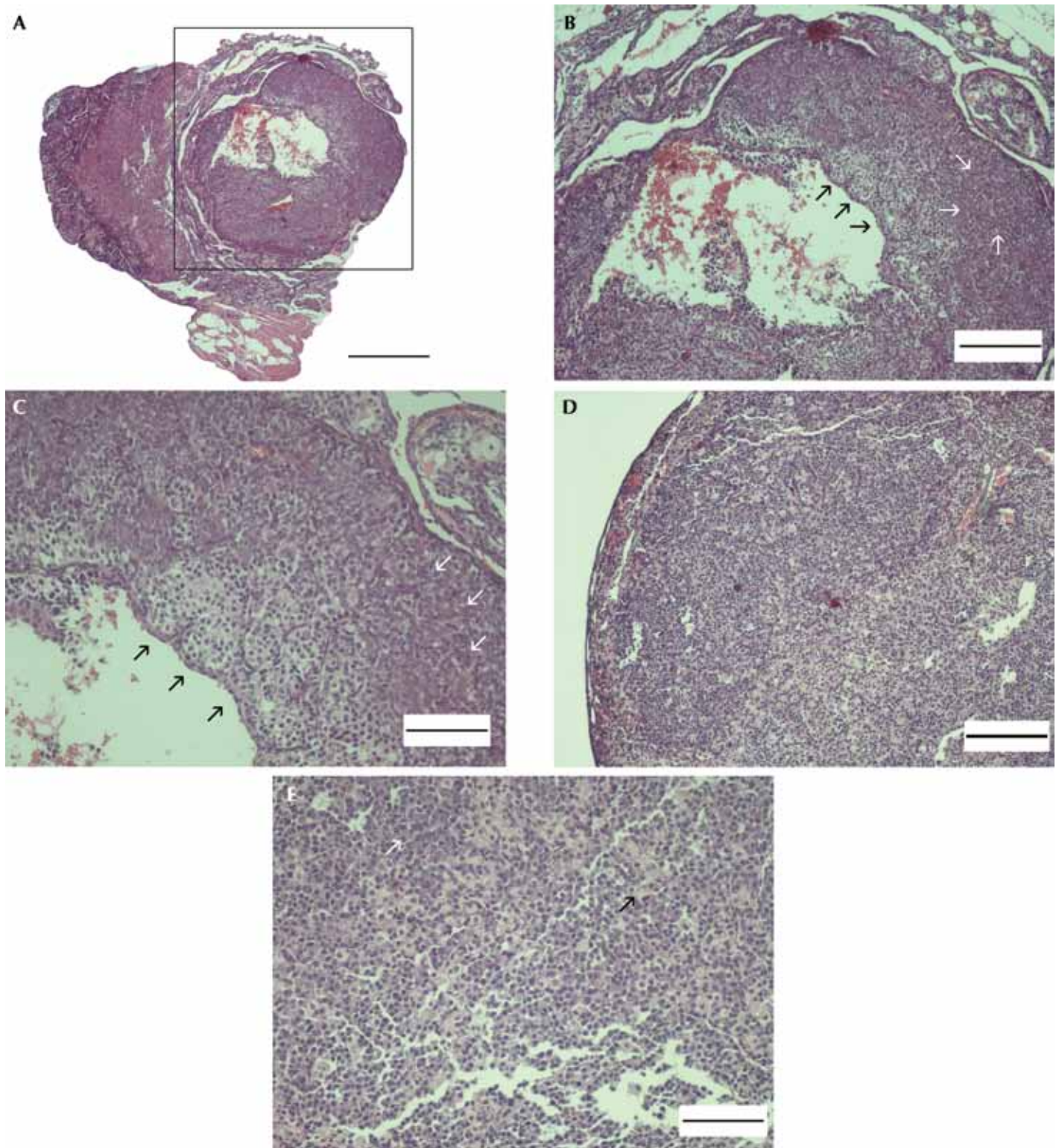


Figure 3. Sections from tumor-containing ovaries at 5 mo after injection. (A) VCD+DMBA+ ovary shows a large Sertoli-Leydig-cell tumor (black square; magnification, $\times 4$). (B and C) Higher-magnification images (B, magnification: $\times 10$; C, magnification, $\times 20$) showing the Sertoli- (white arrows) and Leydig cell-like (black arrows) components of the tumor shown in panel A. (D) VCD+DMBA+ ovary with Sertoli-Leydig-cell tumor where Sertoli-like cells have invaded the entire ovary (same as shown in Figure 2 F). Magnification, $\times 10$. (E) Higher-magnification image ($\times 20$) of ovary in panel D showing the Sertoli- (white arrows) and Leydig- (black arrows) like components. Hematoxylin and eosin stain. Scale bars: A, 500 μm ; B and D, 200 μm ; and C and E, 100 μm .

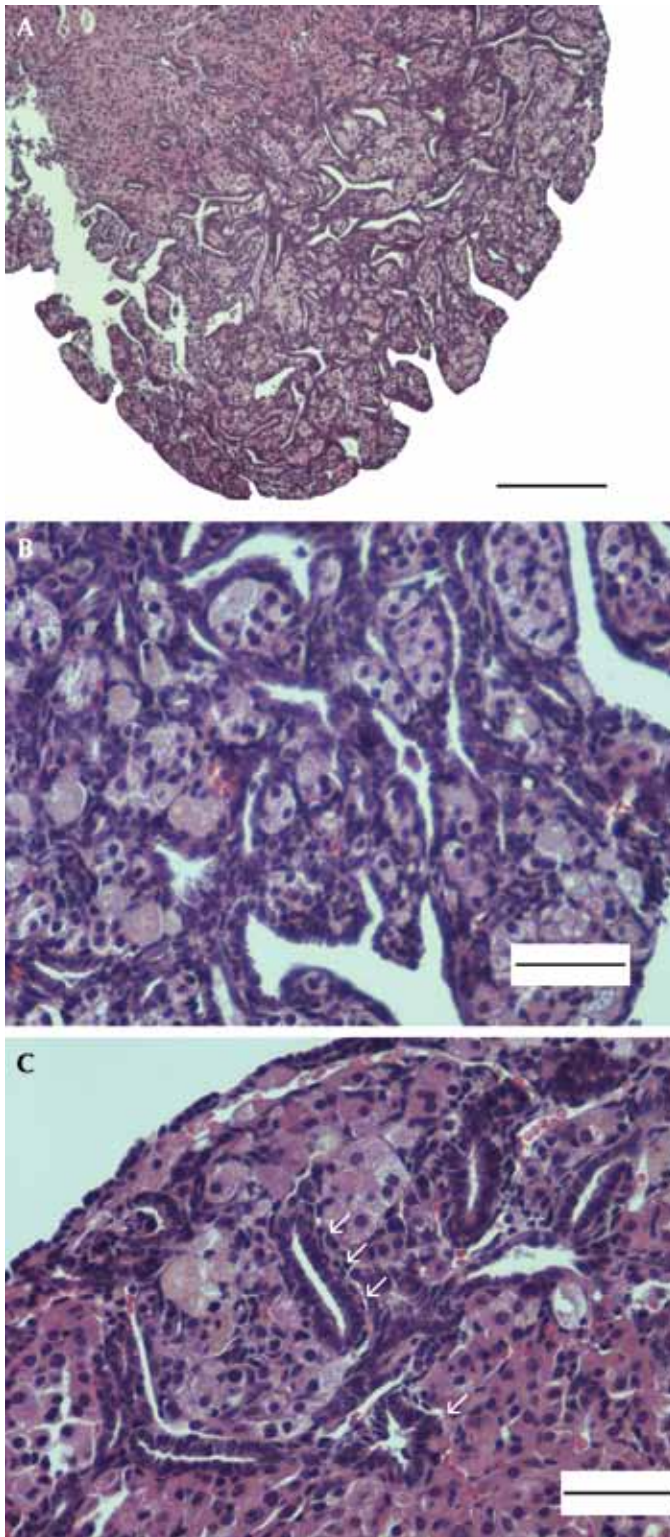


Figure 4. Sections from ovaries containing tubular adenomas at 3 mo after injection. (A) Ovary containing a tubular adenoma (magnification, $\times 10$; bar, 200 μm). (B) Same tumor as in panel A (magnification, $\times 20$; bar, 100 μm). (C) Tubular adenoma with inclusion cysts (magnification, $\times 40$; bar, 100 μm). White arrowhead shows the presence of inclusions. The larger pink cells are background luteinized stromal cells. Hematoxylin and eosin stain.

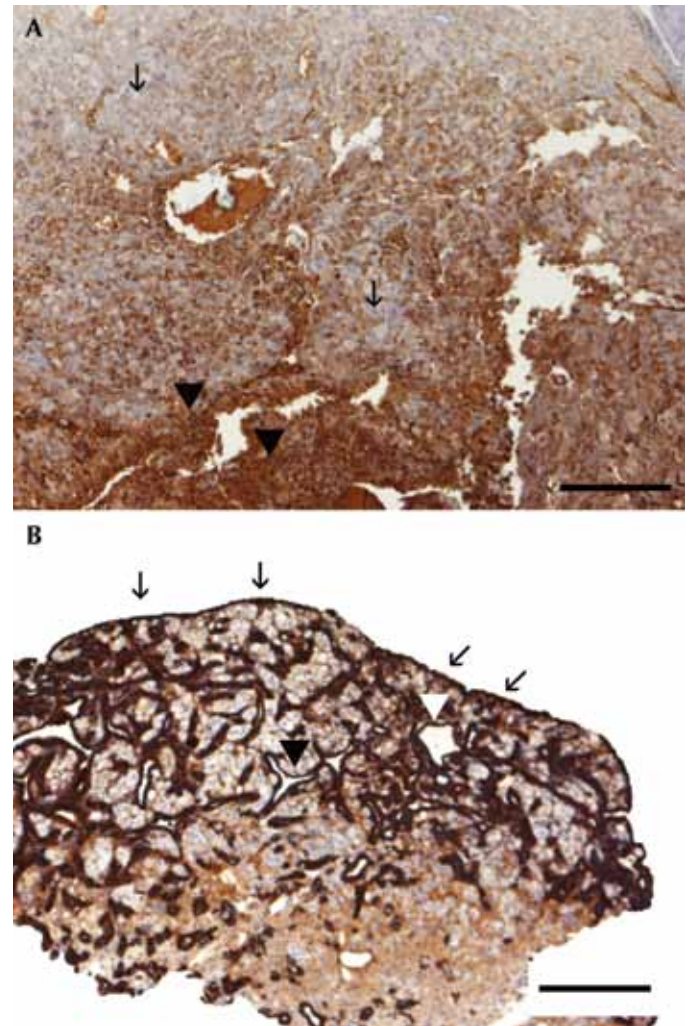


Figure 5. Immunohistochemical staining of ovarian neoplasms present in VCD-treated follicle-depleted ovaries 5 mo after intrabursal injection with DMBA. All ovaries are from VCD+DMBA+ mice with Sertoli-Leydig-cell tumors. (A) Tumor with strong dark-brown staining for inhibin α in Sertoli-like cells (black arrowheads) and weak or absent staining in Leydig-like cells (black thin arrows). (B) Tubular adenoma showing dark-brown positive staining for keratin 7 (black thin arrows) and background luteinized stromal cells lacking staining but with inclusions (arrowheads). Magnification, $\times 10$; bar, 200 μm .

tential stimulation to the ovarian stroma) that accompany ovarian failure. Depletion of ovarian follicles and oocytes has been hypothesized to cause ovarian tumors in animal models of premature ovarian failure.⁴⁶ Therefore, because the current study represents the first time that DMBA-induced ovarian neoplasms have been induced in follicle-depleted mice, the number of tumor cases among VCD+DMBA- mice may represent a baseline incidence for ovarian neoplasms in mice with ovarian failure rather than as a direct effect of previous VCD exposure.

Alternatively, increased expression of microsomal epoxide hydrolase mRNA (*Ephx1* or *mEH*) is highly enriched in the residual ovarian tissue of VCD-treated follicle-depleted mice when compared with age-matched cycling controls.³⁸ The epoxide hydrolase 1 enzyme, together with CYP1A1 and CYP1B1, is involved in the bioactivation pathway of DMBA to its final ovotoxic 3,4-diol-

1,2-epoxide metabolite.^{11,31} Although epoxide hydrolase 1 is not the rate-limiting enzyme in this pathway, its increased levels in VCD-treated follicle-depleted ovaries may impart increased susceptibility to toxicity by DMBA. Furthermore, the possibility that VCD acts as an initiating agent that makes ovarian tissue more susceptible to developing neoplasms must also be considered.

Ovarian cancer has been termed a disease of the postmenopausal stage²² because the incidence increases with age and peaks during the postmenopausal years.¹² Among the risk factors for ovarian cancer are germ cell depletion, increased levels of gonadotropins, and altered levels of estrogens and androgens.⁴¹ These risk factors develop or undergo marked changes during and after the menopausal transition^{3,4,41} and occur in VCD-treated mice as they undergo ovarian failure.^{24,25,27} One interesting finding from the current study is the presence of invaginations of the ovarian surface epithelium in both ovaries of all VCD-treated follicle-depleted animals (benign tubular adenomas). This phenomenon has been described previously in both humans⁴⁰ and animal models with premature ovarian failure.^{17,32,34,47} Studies in W^x/W^y (which have altered *Kit* genes^{30,37}) and Sl/Sl^t and Sl/Sl^d mice (which have mutant *Kitl* genes^{7,17}) show that these mice undergo premature ovarian failure accompanied by changes in OSE morphology and increased stromal invagination^{17,32,47} leading to tubular adenomas. In those animals, lack of follicles leads to decreased levels of estrogen and progesterone, resulting in decreased negative feedback on the secretion of luteinizing and follicle-stimulating hormones and causing their levels to rise.³³ High levels of luteinizing hormone can lead to increased stimulation of the stromal compartment, stromal cell hypertrophy, and luteinization. Furthermore, advanced ovarian failure in mice leads to migration of OSE cells into the ovarian stroma and altered epithelial-stromal cell interactions. These changes are thought to result in increased susceptibility to malignant transformation⁴⁶ by stimulation of OSE cells by androgens produced from tubular adenomas.⁴⁵ Moreover, an increased incidence of OSE pseudostratification, papillomatosis, deep cortical invaginations, epithelial inclusion cysts, and increased stromal activity has been noted in women with a family history of ovarian cancer when compared with women with no history of the disease.⁴⁰ Therefore, the observation of benign tubular adenomas in both ovaries of VCD-treated follicle-depleted mice (with or without DMBA treatment) supports the idea that this phenomenon is associated with ovarian failure and that these changes may precede ovarian neoplasia in these mice.

In summary, results of this study support previous reports predicting an increased risk for the development of ovarian neoplasms after ovarian failure. Compared with that in cycling animals, follicle depletion and the resulting altered hormonal milieu may predispose mice to the development of ovarian neoplasms. Although our mice did not develop neoplasms of epithelial origin (the most common ovarian tumors in humans), the marked stratification of OSE cells and invaginations of OSE cells into the stromal compartment (tubular adenomas) present in VCD-treated follicle-depleted mice indicate potential early changes leading to future neoplasms. All tumors observed in this study were Sertoli-Leydig-cell tumors, thus providing a mouse model for postmenopausal sex-cord-stromal tumors of the Sertoli-Leydig type. Therefore, the present study supports a relevant contribution of the VCD-treated mouse model to the study of ovarian cancer as a menopause-related pathology.

Acknowledgments

The authors thank Patricia J Christian Nivedita Sen, and Aileen F Keating for help with animal handling. Help provided by Dr Heddwyn L Brooks and Andrea Grantham is greatly appreciated. This research was funded by NIH AG021948 and ES06694 to PBH, NIH CA119200 to JKB, and an American Physiological Society Porter Physiology Fellowship to ZRC.

References

1. Alison RH, Morgan KT. 1987. Ovarian neoplasms in F344 rats and B6C3F1 mice. *Environ Health Perspect* 73:91-106.
2. American Cancer Society. [Internet]. Ovarian cancer. [Cited Oct 2006]. Available at <http://documents.cancer.org/114.00/114.00.pdf>.
3. Birken S, O'Connor J, Kovalevskaya G, Lobel L. 2000. Gonadotropins and menopause: new markers, p 61-73. In: Lobo RA, Kelsey J, Marcus R, editors. *Menopause: biology and pathobiology*. San Diego (CA): Academic Press.
4. Burger HG. 2000. Perimenopausal changes in FSH, the inhibins, and the circulating steroid hormone milieu, p 147. In: Lobo RA, Kelsey J, Marcus R, editors. *Menopause: biology and pathobiology*. San Diego (CA): Academic Press.
5. Buters J, Quintanilla-Martinez L, Schober W, Soballa VJ, Hintermair J, Wolff T, Gonzalez FJ, Greim H. 2003. CYP1B1 determined susceptibility to low doses of 7,12-dimethylbenz[a]anthracene-induced ovarian cancers in mice: correlation of CYP1B1-mediated DNA adducts with carcinogenicity. *Carcinogenesis* 24:327-334.
6. Colombo N, Van Gorp T, Parma G, Amant F, Gatta G, Sessa C, Vergote I. 2006. Ovarian cancer. *Crit Rev Oncol Hematol* 60:159-179.
7. Copeland NG, Gilbert DJ, Cho BC, Donovan PJ, Jenkins NA, Cosman D, Anderson D, Lyman SD, Williams DE. 1990. Mast cell growth factor maps near the steel locus on mouse chromosome 10 and is deleted in a number of steel alleles. *Cell* 63:175-183.
8. Crist KA, Zhang Z, You M, Gunning WT, Conran PB, Steele VE, Lubet RA. 2005. Characterization of rat ovarian adenocarcinomas developed in response to direct instillation of 7,12-dimethylbenz[a]anthracene (DMBA)-coated suture. *Carcinogenesis* 26:951-957.
9. Daniel FB, Joyce NJ. 1984. 7,12-dimethylbenz[a]anthracene-DNA adducts in Sprague-Dawley and Long-evans female rats: the relationship of DNA adducts to mammary cancer. *Carcinogenesis* 5:1021-1026.
10. Danilovich N, Roy I, Sairam MR. 2001. Ovarian pathology and high incidence of sex cord tumors in follitropin receptor knockout (FORKO) mice. *Endocrinology* 142:3673-3684.
11. Gonzalez FJ. 2001. The use of gene knockout mice to unravel the mechanisms of toxicity and chemical carcinogenesis. *Toxicol Lett* 120:199-208.
12. Horner MJ, Ries LAG, Krapcho M, Neyman N, Aminou R, Howlander N, Altekruse SE, Feuer EJ, Huang L, Mariotto A, Miller BA, Lewis DR, Eisner MP, Stinchcomb DG, Edwards BK, editors. 2009. [Internet]. SEER Cancer Statistics Review, 1975-2006, National Cancer Institute. Based on November 2008 SEER data submission, posted to the SEER web site. [Cited May 2009]. Available at http://www.seer.cancer.gov/csr/1975_2006/index.html.
13. Hoyer PB, Davis JR, Bedrnicek JB, Marion SL, Christian PJ, Barton JK, Brewer MA. 2009. Ovarian neoplasm development by 7,12-dimethylbenz[a]anthracene (DMBA) in a chemically-induced rat model of ovarian failure. *Gynecol Oncol* 112:610-615.
14. Hu X, Christian PJ, Sipes IG, Hoyer PB. 2001. Expression and redistribution of cellular bad, bax, and bcl-X(L) protein is associated with VCD-induced ovotoxicity in rats. *Biol Reprod* 65:1489-1495.
15. Hu X, Christian PJ, Thompson KE, Sipes IG, Hoyer PB. 2001. Apoptosis induced in rats by 4-vinylcyclohexene diepoxide is associated with activation of the caspase cascade. *Biol Reprod* 65:87-93.
16. Institute of Laboratory Animal Resources. 1996. Guide for the care and use of laboratory animals. Washington (DC): National Academies Press.

17. **Ishimura K, Matsuda H, Tatsumi H, Fujita H, Terada N, Kitamura Y.** 1986. Ultrastructural changes in the ovaries of *Sl/Sl* mutant mice, showing developmental deficiency of follicles and tubular adenomas. *Arch Histol Jpn* **49**:379–389.
18. **Judson PL, Boente MP.** 2003. Ovarian sex cord–stromal tumors, p 231. In: Ozols RF, editor. *Ovarian cancer*. Hamilton (Canada): BC Decker.
19. **Kanter EM, Walker RM, Marion SL, Brewer M, Hoyer PB, Barton JK.** 2006. Dual modality imaging of a novel rat model of ovarian carcinogenesis. *J Biomed Opt* **11**:041123.
20. **Keck M, Romero-Aleshire MJ, Cai Q, Hoyer PB, Brooks HL.** 2007. Hormonal status affects the progression of STZ-induced diabetes and diabetic renal damage in the VCD mouse model of menopause. *Am J Physiol Renal Physiol* **293**:F193–F199.
21. **Krarup T.** 1969. Oocyte destruction and ovarian tumorigenesis after direct application of a chemical carcinogen (9:10-dimethyl-1:2-benzanthrene) to the mouse ovary. *Int J Cancer* **4**:61–75.
22. **Kufe DW, Pollock RE, Weichselbaum RR, Bast RC, Gansler TS, Holland JF, Fre E 3rd.** 2003. *Cancer medicine*. Hamilton (Canada): BC Decker.
23. **Kuwahara I.** 1967. Experimental induction of ovarian tumors in mice treated with single administration of 7,12-dimethylbenz[*a*]anthracene, and its histopathological observation. *Gann* **58**:253–266.
24. **Lohff JC, Christian PJ, Marion SL, Arrandale A, Hoyer PB.** 2005. Characterization of cyclicity and hormonal profile with impending ovarian failure in a novel chemical-induced mouse model of perimenopause. *Comp Med* **55**:523–527.
25. **Lohff JC, Christian PJ, Marion SL, Hoyer PB.** 2006. Effect of duration of dosing on onset of ovarian failure in a chemical-induced mouse model of perimenopause. *Menopause* **13**:482–488.
26. **Mattison DR, Schulman JD.** 1980. How xenobiotic chemicals can destroy oocytes. *Contemp Obstet Gynecol* **15**:157–169.
27. **Mayer LP, Devine PJ, Dyer CA, Hoyer PB.** 2004. The follicle-deplete ovary produces androgen. *Biol Reprod* **71**:130–138.
28. **Mayer LP, Dyer CA, Eastgard RL, Hoyer PB, Banka CL.** 2005. Atherosclerotic lesion development in a novel ovary-intact mouse model of perimenopause. *Arterioscler Thromb Vasc Biol* **25**:1910–1916.
29. **McCluggage WG.** 2002. Recent advances in immunohistochemistry in gynaecological pathology. *Histopathology* **40**:309–326.
30. **Mintz B, Russell ES.** 1957. Gene-induced embryological modifications of primordial germ cells in the mouse. *J Exp Zool* **134**:207–237.
31. **Miyata M, Kudo G, Lee YH, Yang TJ, Gelboin HV, Fernandez-Salguero P, Kimura S, Gonzalez FJ.** 1999. Targeted disruption of the microsomal epoxide hydrolase gene. microsomal epoxide hydrolase is required for the carcinogenic activity of 7,12-dimethylbenz[*a*]anthracene. *J Biol Chem* **274**:23963–23968.
32. **Murphy ED.** 1972. Hyperplasia and early neoplastic changes in the ovaries of mice after genic deletion of germ cells. *J Natl Cancer Inst* **48**:1283–1295.
33. **Murphy ED, Beamer WG.** 1973. Plasma gonadotropin levels during early stages of ovarian tumorigenesis in mice of the *W^wW^w* genotype. *Cancer Res* **33**:721–723.
34. **Murphy ED, Russell ES.** 1963. Ovarian tumorigenesis following genic deletion of germ cells in hybrid mice. *Acta Unio Int Contra Cancrum* **19**:779–782.
35. **Nicol CJ, Yoon M, Ward JM, Yamashita M, Fukamachi K, Peters JM, Gonzalez FJ.** 2004. PPAR γ influences susceptibility to DMBA-induced mammary, ovarian, and skin carcinogenesis. *Carcinogenesis* **25**:1747–1755.
36. **Prejean JD, Peckham JC, Casey AE, Griswold DP, Weisburger EK, Weisburger JH.** 1973. Spontaneous tumors in Sprague–Dawley rats and Swiss mice. *Cancer Res* **33**:2768–2773.
37. **Reith AD, Rottapel R, Giddens E, Brady C, Forrester L, Bernstein A.** 1990. *W*-mutant mice with mild or severe developmental defects contain distinct point mutations in the kinase domain of the *c-kit* receptor. *Genes Dev* **4**:390–400.
38. **Rivera Z, Hoying JB, Hoyer PB.** 2008. Residual ovarian tissue of follicle-depleted mice expresses genes for androgen synthesis and metabolism of xenobiotic compounds. *Biol Reprod* **78**:112.
39. **Romero-Aleshire MJ, Diamond-Stanic MK, Hasty AH, Hoyer PB, Brooks HL.** 2009. Loss of ovarian function in the VCD mouse model of menopause leads to insulin resistance and a rapid progression into the metabolic syndrome. *Am J Physiol Regul Integr Comp Physiol* **297**:R587–R592.
40. **Salazar H, Godwin AK, Daly MB, Laub PB, Hogan WM, Rosenblum N, Boente MP, Lynch HT, Hamilton TC.** 1996. Microscopic benign and invasive malignant neoplasms and a cancer-prone phenotype in prophylactic oophorectomies. *J Natl Cancer Inst* **88**:1810–1820.
41. **Salehi F, Dunfield L, Phillips KP, Krewski D, Vanderhyden BC.** 2008. Risk factors for ovarian cancer: an overview with emphasis on hormonal factors. *J Toxicol Environ Health B Crit Rev* **11**:301–321.
42. **Springer LN, McAsey ME, Flaws JA, Tilly JL, Sipes IG, Hoyer PB.** 1996. Involvement of apoptosis in 4-vinylcyclohexene diepoxide-induced ovotoxicity in rats. *Toxicol Appl Pharmacol* **139**:394–401.
43. **Stewart SL, Querec TD, Ochman AR, Gruver BN, Bao R, Babb JS, Wong TS, Koutroukides T, Pinnola AD, Klein-Szanto A, Hamilton TC, Patriotis C.** 2004. Characterization of a carcinogenesis rat model of ovarian preneoplasia and neoplasia. *Cancer Res* **64**:8177–8183.
44. **Takai Y, Cannign J, Perez GI, Pru JK, Schlezinger JJ, Sherr DH, Kolesnick RN, Yuan J, Flavell RA, Korsmeyer SJ, Tilly JL.** 2003. Bax, caspase 2, and caspase 3 are required for ovarian follicle loss caused by 4-vinylcyclohexene diepoxide exposure of female mice in vivo. *Endocrinology* **144**:69–74.
45. **Terada N, Kitamura Y, Namiki M, Kuroda H, Ito M, Takatsuka D, Matsumoto K.** 1984. Production of androgens and estrogens by tubular adenomas which developed in ovaries of mutant mice of *Sl/Sl* genotype. *Cancer Res* **44**:1827–1830.
46. **Vanderhyden BC.** 2005. Loss of ovarian function and the risk of ovarian cancer. *Cell Tissue Res* **322**:117–124.
47. **Vanderhyden BC, Shaw TJ, Ethier J.** 2003. Animal models of ovarian cancer. *Reprod Biol Endocrinol* **1**:67.
48. **Wang Y, Zhang Z, Lu Y, Yao R, Jia D, Wen W, LaRegina M, Crist K, Lubet R, You M.** 2008. Enhanced susceptibility to chemical induction of ovarian tumors in mice with a germline p53 mutation. *Mol Cancer Res* **6**:99–109.
49. **Weiss NS, Homonchuk T, Young JLJ.** 1977. Incidence of the histological types of ovarian cancer: the US Third National Cancer Survey, 1969–1971. *Gynecol Oncol* **5**:161–167.
50. **Williams JK.** 2005. A mouse model of the perimenopausal transition: importance for cardiovascular research. *Arterioscler Thromb Vasc Biol* **25**:1765–1766.
51. **Wright LE, Christian PJ, Rivera Z, Van Alstine WG, Funk JL, Boussein ML, Hoyer PB.** 2008. Comparison of skeletal effects of ovariectomy versus chemical-induced ovarian failure in mice. *J Bone Miner Res* **23**:1296–1303.